An eight-state molecular sequential switch featuring a dual single-bond rotation photoreaction

Aaron Gerwien,[§] *Benjamin Jehle,*[§] *Marvin Irmler,*[§] *Peter Mayer,*[§] *Henry Dube*[†]*

[§] Ludwig-Maximilians Universität München, Department of Chemistry and Center for Integrated Protein Science CIPSM, Butenandtstr. 5–13, 81377 Munich, Germany

[†] Friedrich-Alexander Universität Erlangen-Nürnberg, Department of Chemistry and Pharmacy, Nikolaus-Fiebiger-Str. 10, 91058 Erlangen, Germany

* E-mail: henry.dube@fau.de

Abstract

Typical photowitches interconvert between two different states by simple isomerization reactions, which represents a fundamental limit for applications. To expand the switching capacity usually different photoswitches have to be linked together leading to strong increase in molecular weight, diminished switching function, and less precision and selectivity of switching events. Herein we present an approach for solving this essential problem with a different photoswitching concept. A basic molecular switch architecture provides precision photoswitching between eight different states via controlled rotations around three adjacent covalent bonds. All eight states can be populated one after another in an eight-step cycle by alternating between photochemical Hula-Twist isomerizations and thermal single bond rotations. By simply changing solvent and temperature the same switch can also undergo a different cycle instead interconverting just five isomers in a selective sequence. This behavior is enabled through the discovery of an unprecedented photoreaction, a one photon dual single bond rotation.

Introduction

Molecular photoswitches are at the center of attention in smart nanotechnology research enabling high precision control of events at the smallest scales and instilling bottom-up responsiveness and adaptability into materials, drugs, or catalytic reactions. Consequentially photoswitches are used for switching or gradual modulation of functions in myriads of applications nowadays and developments are ever steeply increasing.[1-16] Roughly two different classes of photoswitches can be distinguished, bond isomerizing switches that undergo significant changes in molecular geometry and switches that provide substantial changes in their electronic structure.[6, 13, 17, 18] The overwhelming majority of light induced bond isomerizations are achieved by simple one-bond rotations such as double bond isomerization (DBI) reactions.[8, 12, 19-21] Direct experimental proof for more complex coupled bond isomerizations, where more than one bond rotates concomitantly, are so far only available for bicycle pedal[22] and Hula Twist photoreactions[23, 24] (Figure 1a) although such simultaneous photochemical processes are proposed frequently in the literature.[25-32]

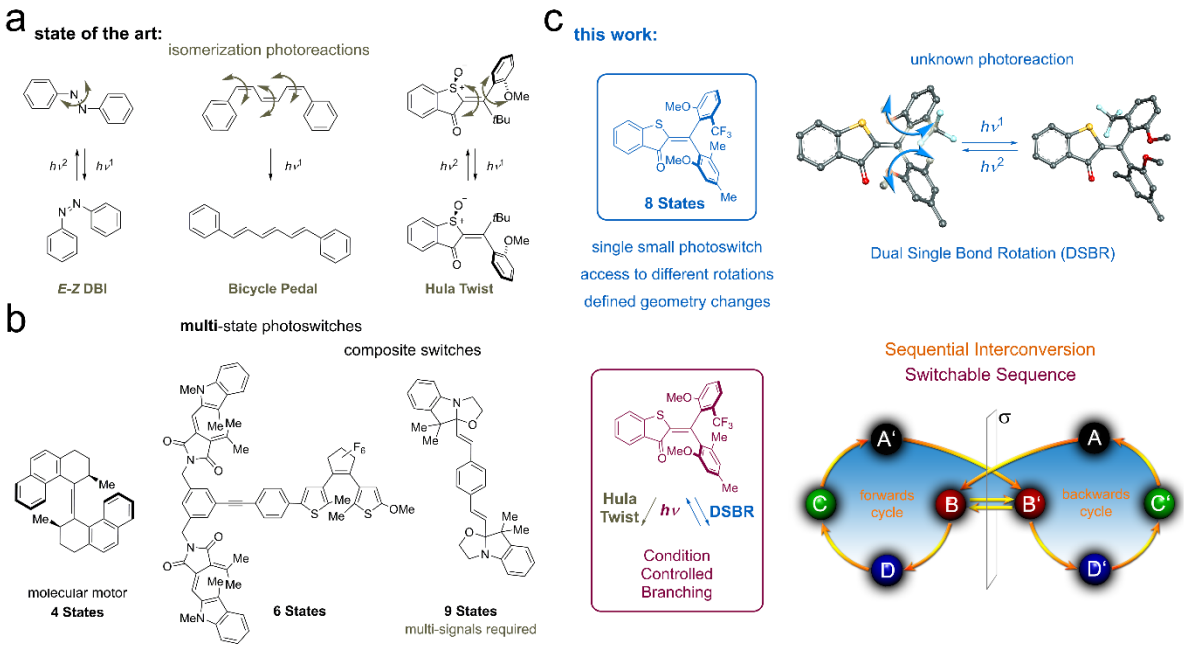

Figure 1 Molecular photoswitching. a) Bond rotations currently evidenced in photoswitching. b) Multi-state switching approaches. c) Simple and compact 8-state photoswitch with switchable sequential interconversion employing a hitherto unknown dual single bond rotation (DSBR) and Hula Twist photoreactions.

At the current state of the art most small molecular photoswitches can undergo reversible changes between two different states upon irradiation with light. To go beyond this binary behavior and open up more fundamental switching possibilities (Figure 1b), multiple photo responsive units can be incorporated into a single larger molecule. This is achieved by linking either the same or different photochromic units together in a covalent fashion or through weaker interactions.[16, 33-38] Many well-

known photoswitches like azobenzene,[37, 39-43] diarylethene,[44-47] or spiropyranes[48] have been interlinked in such a manner but the method can be extended to virtually any photochromic dye[34, 35, 49] or dye-combination.[50-52] An impressive escalation in the number of switching states is thus achievable, for example six different states are possible by connecting three light-responsive units covalently into one structure.[51] Another possibility to enhance the switching state number for a given photochromic molecule is provided by adding chemical signals like protonation and deprotonation.[7, 53-55] Alternatively, photon driven molecular motors can be considered as compact multi-state photoswitches,[56-59] usually operating by alternating four different diastereomeric states.[56, 60-65] The advantage of the latter is their unequivocally more precise geometry control as opposed to the oftentimes rather loose changes obtained in multi-component architectures. We recently contributed different types of visible light driven molecular motors to the field, featuring different rotation mechanisms and alternating between three to four different states.[24, 63, 66] Up to five distinct states could be accessed in macrocyclic integrated hemithioindigo (HTI) motors.[67] Despite this steep progress in molecular photoswitches research, controlling more complex motions and using the full state-density capacity offered by small molecular frameworks remain untackled challenges at present.

Herein we report on a simple and compact molecular setup **1** assuming eight different stable states, which interchange one after another by alternating visible light irradiation and heating steps. The photochemical steps encompass a variant of the Hula Twist photoreaction as well as a hitherto unknown dual single bond rotation (DSBR) photoreaction (Figure 1c). The thermal steps are sole single bond rotations (SBRs). Change of the solvent polarity enables to control the sequence of isomer interconversions and either eight or five states are interchanged under irradiation and heating in specific sequences. With this compact multi-state photoswitch architecture the next level in molecular addressability has been achieved providing exquisite control over precise molecular geometry changes via light signaling. At the same time a so far unknown coupled photoisomerization reaction is discovered, which provides molecular scientists with a novel light-inducible molecular motion type.

Results and discussion

Sequential switch **1** is derived from the parent HTI chromophore but contains two different aryl groups geminally connected to the photoisomerizable double bond. Both aryl groups are nonsymmetrically substituted thus establishing a chiral axis each, which coincides with the respective single bond connecting to the central double bond. Therefore, sequential switch **1** exists in four diastereomeric states and eight enantiomeric states. All states of **1** - denoted **A** (*Z*-(S_a)-(R_a) configuration), enantiomeric **A'** *(Z*-(R_a)-(S_a) configuration), **B** (*Z*-(R_a)-(R_a) configuration), enantiomeric **B'** (*Z*-(S_a)-(S_a) configuration), **C** (*E*-(R_a)-(R_a) configuration), enantiomeric **C'** (*E*-(S_a)-(S_a) configuration), **D** (*E*-(R_a)-(S_a) configuration), and enantiomeric **D'** (*E*-(S_a)-(R_a) configuration) are depicted in Figure 2a.

Synthesis of **1** followed an established protocol for the generation of fourfold double-bond substituted HTIs (see Supporting Information).[68] Because of increased steric hindrance of the two aryl substituents all atropisomers show increased thermal stability facilitating isolation and analysis. Isomers *rac*-**A** and *rac*-**B** are stable enough at 22 °C to enable separation by chromatography methods. Isomers *rac*-**C** and *rac*-**D** are interconverting rapidly at 22 °C making a separation impossible. However, since isomer *rac*-**C** is significantly more stable, it is mainly populated at ambient temperatures as confirmed by NMR spectroscopy. Consequentially it is also the only isomer, which crystallizes from a solution of *rac*-**C** and *rac*-**D** isomers and can thus be obtained in highly enriched form. These results are in good agreement with the theoretical description predicting isomers *rac*-**D** to be 0.63 kcal/mol higher in energy as compared to *rac*-**C** (see Figure 3 and the Supporting Information).

The relative configurations of the different diastereomers were elucidated by 1D and 2D-NMR methods in combination with crystal structure analysis by X-ray diffraction (see Figure 2b and Supporting Information). The absolute configurations could be revealed after separation of the enantiomers by chiral HPLC and comparison of experimentally obtained ECD-spectra with calculated ECD spectra (B3LYP/6-311G(d,p) level of theory using a PCM solvent model for MeCN). The structural assignments were confirmed by X-ray crystal structure analysis of racemic **A**/ **A'**, **B**/ **B'**, and **C**/ **C'** and enantiopure **C'** and **C** isomers (see Figure 2b and c, and Supporting Information).

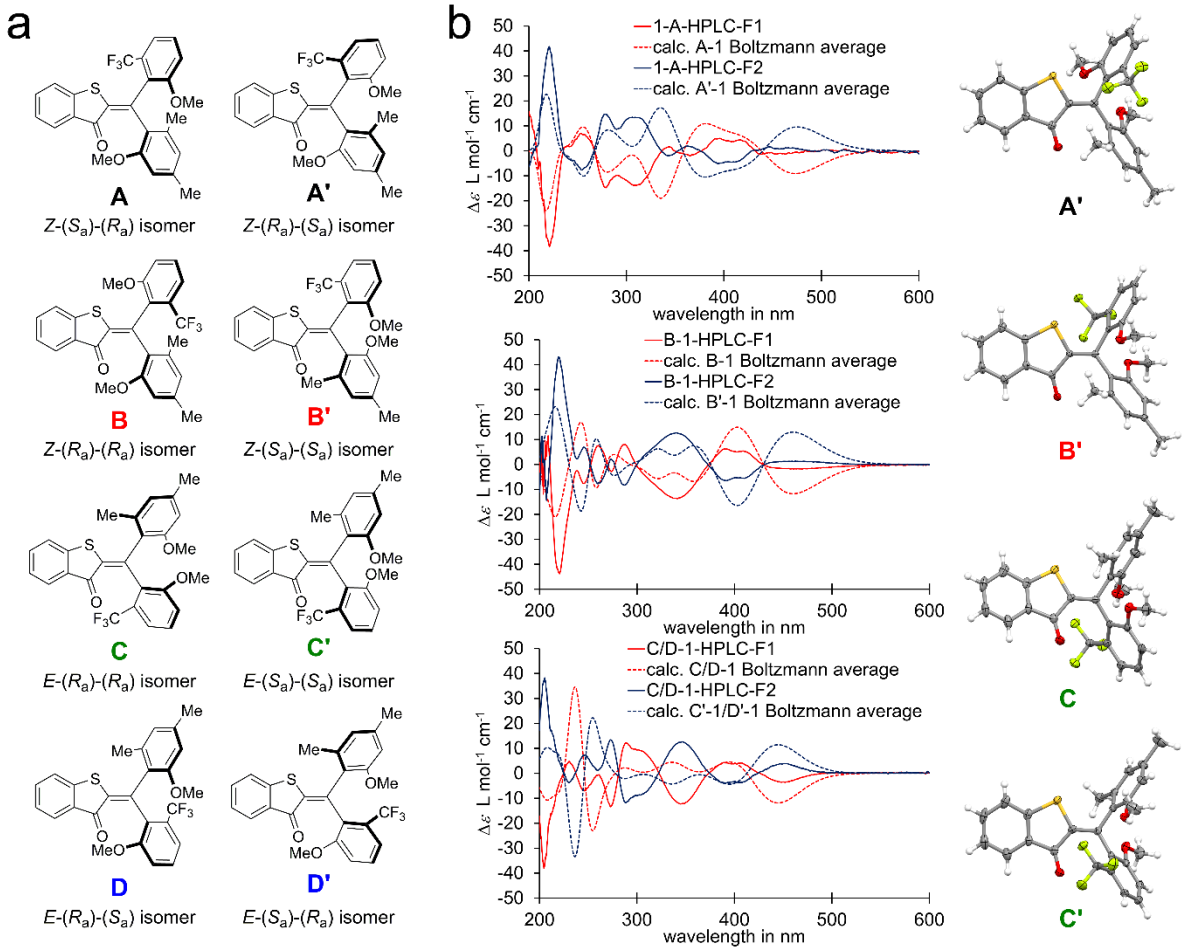

Figure 2 Structures of all eight isomers of sequential HTI switch **1** and corresponding ECD-spectra of enantiomerically pure samples. a) Schematic representation of the molecular structures of **1** with stereo labels. b) Structures of isomers **A'** (from racemic crystals), **B'** (from racemic crystals), **C'**, and **C** in the crystalline state and corresponding ECD-spectra in MeCN at 20 °C of **A**, **A'**, **B**, **B'**, **C/D**, **C'/D'**. Experimental spectra were compared with calculated spectra (B3LYP/6-311G(d,p) level of theory using a PCM solvent model for MeCN).

Thermal isomerization reactions and the ground state energy profile of HTI **1** and its different isomers were determined in a combined theoretical (B3LYP/6-311G(d,p) level of theory using a PCM solvent model for MeCN) and experimental approach as summarized in Figure 3. The relative Gibbs free energies ΔG of the stable isomers were determined experimentally by heating a sample of **1** to 62 °C over prolonged time in MeCN-d_3 solution to establish thermal equilibrium (Figure 3a and b). From the relative abundance of each enantiomeric pair *rac*-**A** to *rac*-**D** the corresponding ΔG value could be obtained (see Supporting Information). The Gibbs energy of activation for thermal atropisomerization of *rac*-**A** to *rac*-**B** was determined to be $\Delta G^{\ddagger}$ = 26.8 kcal mol^{-1} in MeCN-d_3 solution by following its thermal decay at 62 °C with ^{1}H NMR spectroscopy. The theoretical description predicts isomer interconversion by selective rotation of the trifluormethylanisol substituent whereby the methoxy substituent faces the side of the sulfur atom (TS2, Figure 3c). The selective rotation of one aromatic ring was confirmed by following the atropisomerization of enantiomers by chiral HPLC (see Figure 3a and Supporting Information for details). Isomer **A** is thermally converted exclusively into isomer **B** and **A'** is thermally converted exclusively into **B'**. This selectivity is only possible by sole rotation around the trifluormethylanisol substituent. It should be mentioned at this point that a significant energy difference between the two possible transition states TS1 and TS2 is found in the theoretical description. Therefore theory predicts a unidirectional rotation for this atropisomerization, which can however not be proven straightforwardly in an experiment. A strong indication is given by the good agreement between the absolute $\Delta G^{\ddagger}$ values obtained from theory and experiment.

The corresponding Gibbs energy of activation for thermal *rac*-**C**/*rac*-**D** interconversion was found to be $\Delta G^{\ddagger}$ = 18.8 kcal mol^{-1} in MeCN-d_3 solution by following the decay kinetics of a *rac*-**D** enriched sample with low temperature ^{1}H NMR at -20 °C in the dark (see Figure 3b and Supporting Information). The theoretical description predicts that this atropisomerization takes place by sole rotation of the dimethylanisol substituent whereby the methoxy substituent faces the side of the sulfur atom (i.e. via transition state TS5, Figure 3c). The selective rotation could be confirmed experimentally (see Supporting Information). After chiral HPLC separation of the enantiomer pairs **C**/**D** from the pairs **C'**/**D'** at 22 °C thermal interconversion of the enantiopure samples was monitored using chiral HPLC as analytical method. Only thermal conversion of **D** to **C** as well as of **D'** to **C'** is observed after photoinduced enrichment of the **D**/**D'** isomers. Rotation of the trifluormethylanisol substituent would lead to interconversions from **D'** to **C** and **D** to **C'** respectively, which was not observed in the experiments. Again an unidirectional rotation of the single bond is predicted from theory for the

atropisomerization between *rac*-**D** and *rac*-**C**. The thermal isomerization reactions of HTI **1** were thus found to be highly selective and only the aromatic residue with *Z* relation to the sulfur atom rotates in this process. No thermal double bond isomerization was observed even after prolonged heating to 140 °C in tetrachloroethane-d_2 solution and thus the relative stabilities of *Z* and *E* configured isomers could not be determined experimentally.

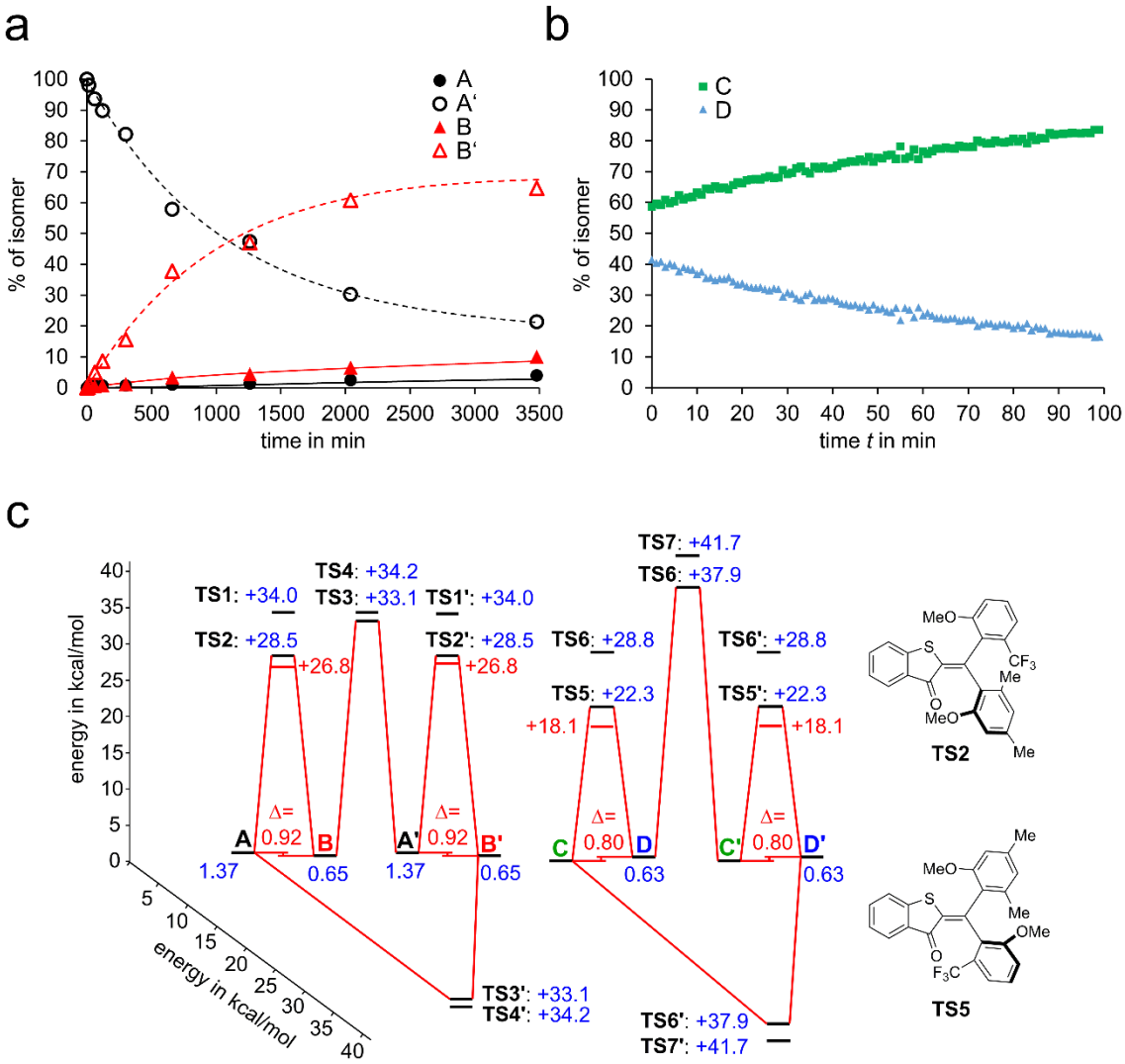

Figure 3 Thermal properties of sequential HTI switch **1**. a) Kinetics of the thermal atropisomerization from **A'** to **B'** in MeCN at 60 °C followed by chiral HPLC. Experimental data were fitted using a Markov matrix kinetic model (see Supporting Information for details). b) Kinetics of the thermal atropisomerization from *rac*-**D** to *rac*-**C** in MeCN-d_3 at -20 °C followed by ^{1}H NMR spectroscopy (400 MHz, -20 °C). c) Ground state energy profile of HTI **1** experimentally determined in MeCN-d_3 solution (red) and calculated at the B3LP/6-311G(d,p) of level of theory with a PCM solvent model for MeCN (blue).

After establishing the thermal behavior of **1** its photochemistry was studied in detail (Figure 4a). Isomers **A**, **A'**, **B**, and **B'** could be isolated in pure form and their photochemical reactions were elucidated individually. Isomers **C/D** and **C'/D'** could only be isolated as enantiomerically pure mixtures of diastereomers at ambient temperatures. Their photochemical properties were thus determined in

thermodynamic equilibrium at 22 °C or separately at low temperatures after selective isomer enrichment. Irradiation of pure *rac*-**A** in MeCN did not lead to significant population of other isomers and therefore productive photochemistry of these enantiomers is strongly subdued. In contrast irradiation of isomers *rac*-**B** in MeCN at -40 °C with 450 nm leads to exclusive formation of *rac*-**D** and a ratio of *rac*-**B** : *rac*-**D** = 52 : 48 is established in the photostationary state (PSS, see Figure 4b and Supporting Information). Because of this PSS composition it was also established that *rac*-**D** only undergoes photoisomerization back to *rac*-**B**. When warming up the solution above -30 °C thermal *rac*-**D** to *rac*-**C** atropisomerization was observed as discussed above. If irradiation was continued at the higher temperature photochemical *rac*-**C** to *rac*-**A** isomerization occurred. In a similar experiment at 22 °C, illumination of an equilibrium *rac*-**D**/*rac*-**C** mixture with 405 nm light resulted in strong accumulation of *rac*-**A** in the PSS with a ratio of *rac*-**A** : *rac*-**B** : *rac*-**C** : *rac*-**D** = 95 : 3 : 2 : 0 (see Figure 4c and Supporting Information). It is thus possible to enrich *rac*-**A** almost quantitatively under irradiation with blue light. Quantum yields for the two photoreactions of *rac*-**B** and *rac*-**C** were obtained using photon counting in conjunction with ^{1}H NMR or UV/vis spectroscopy and chiral HPLC analysis and are discussed further below (also see Supporting Information for more details).

Both photoreactions *rac*-**B** to *rac*-**D** and *rac*-**C** to *rac*-**A** are Hula-Twist reactions, a photoreaction in which the central double bond and one adjacent single bond rotate in the same step.[23, 69] However, the molecular setup of HTI **1** allows for two different Hula-Twist photoreactions for each *rac*-**B** to *rac*-**D** and *rac*-**C** to *rac*-**A** conversion, respectively as such coupled bond rotation can involve either of the two aryl substituents. To elucidate, which single bond is rotated in the Hula-Twist reaction enantiopure samples of **B**, **B'**, **C**/**D**, and **C'**/**D'** were illuminated and the photoreaction kinetics were followed by quantitative ^{1}H NMR or chiral HPLC (see Figure 4b – d, and the Supporting Information). Irradiation of **B** with 450 nm light at -40°C led to formation of **D** in MeCN with a quantum yield of 1.4% while no notable reaction into **D'** was observable (see Figure 4b and d). Thus, the Hula-Twist photoreaction proceeds exclusively by rotation around the central double bond and the single bond connecting to the dimethylanisol substituent. However, another photoreaction was also observed in this experiment leading from **B** to **B'** with a significant quantum yield of 0.9% (Figure 4d). The associated motion is a dual single bond rotation (DSBR) in which two atropisomerization photoreactions occur at the same time, while the central double bond is not isomerized. This reaction is – to the best of our knowledge – not described in the literature. Interestingly, a sole single bond rotation from **B** to **A** or to **A'** was not observed photochemically - if one single bond rotates the other single bond also undergoes rotation. As a result of this dual atropisomerization isomer **B** is converted into its enantiomer **B'**. Isomers **B** and **B'** therefore represent a branching point for the photochemistry of **1**. Full racemization of the sample via DSBR is however prevented since a significant amount of **B** is converted to **D** in the competing Hula Twist photoreaction. As expected, it was found that the enantiomeric isomer **B'** behaves mirror-symmetric and photoisomerizes into **D'** via a Hula-Twist reaction and into **B** via DSBR. Isomer **C** underwent predominantly photoisomerization into **A'** with a quantum yield of 5.2% at 450 nm

irradiation. This corresponds to a Hula-Twist photoreaction involving the central double bond and the adjacent single bond to the dimethylanisol fragment. In this case no DSBR photoreaction or other photoreactions were observed. However, the thermal equilibrium between **C** and **D** accounts for a small population of the **D** isomer in the experiment and therefore photoisomerization of the latter via Hula-Twist to isomer **B** was also detected to some degree. Irradiation of the enantiomeric mixture **C'**/**D'** showed the expected mirror-symmetric behavior and led to population of **A** and small amounts of **B'**, respectively. Finally the photochemistry of both enantiomers **A** and **A'** was scrutinized and (as observed already for the racemic mixture) showed strongly diminished efficiency by at least a factor of 10 compared to photochemical processes that produce **A** and **A'** as products. Some minimal DSBR converting **A** into **A'** and *vice versa* were found together with similarly inefficient conversion to the **C**/**C'** isomers (for details see the Supporting Information).

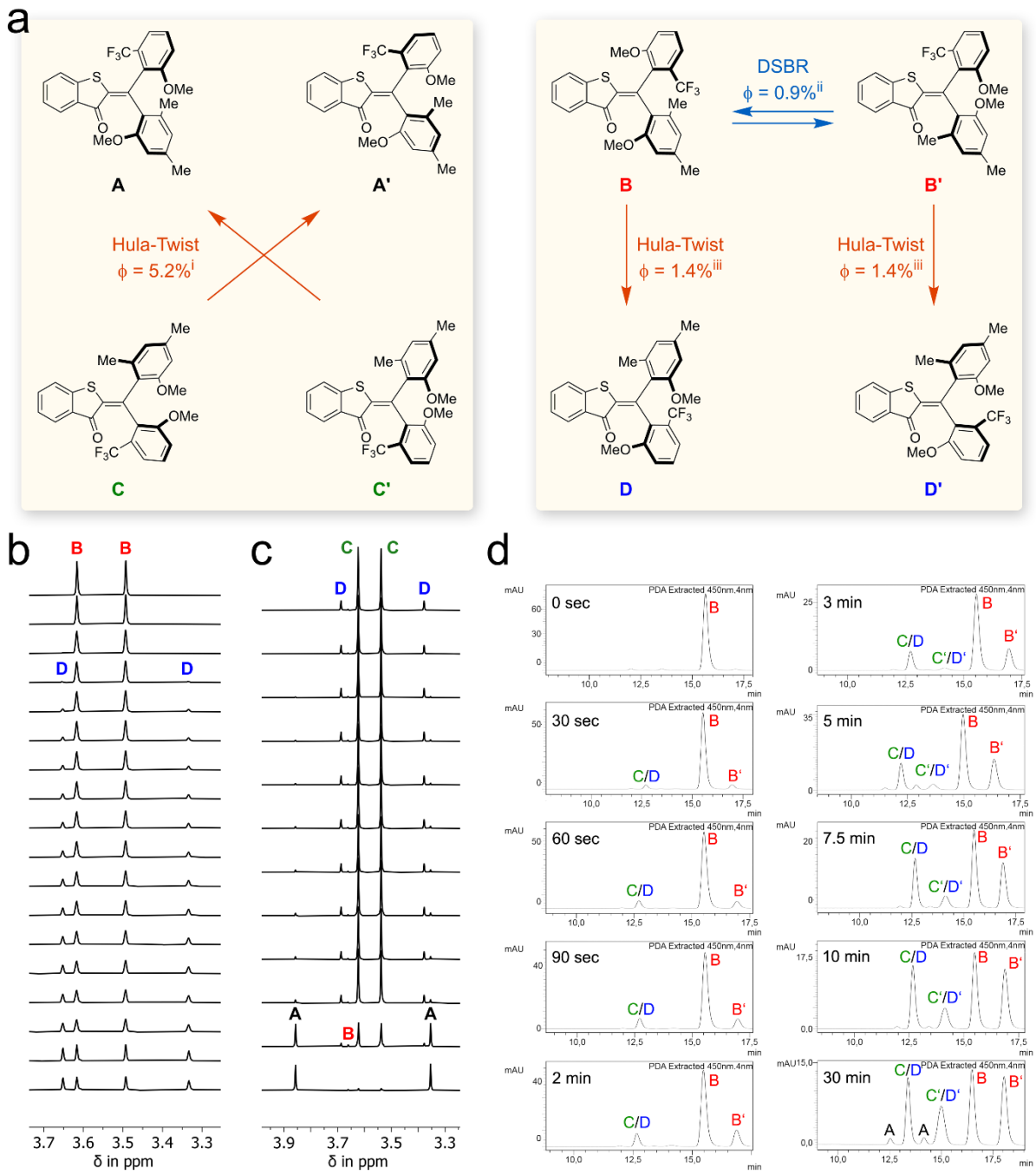

Figure 4 Photoreactions of HTI **1** during 450 nm irradiation. a) Photoreactions of **1** and associated quantum yields measured in MeCN solution. [i] Quantum yield determined taking into account the thermodynamic equilibrium of **C** and **D** at 20 °C. [ii] DSBR = double single bond rotation, quantum yield indirectly determined by multiplying the ratio of the photoproducts determined by chiral HPLC analysis with the quantum yield for the Hula-Twist reaction from *rac*-**B** to *rac*-**D** measured at -40 °C. [iii] Quantum yield determined at -40 °C. b) Photoconversion of isomer *rac*-**B** in MeCN-d_3 solution at -40 °C followed by ^{1}H NMR-spectroscopy (400 MHz). Starting with pure *rac*-**B** (top spectrum) only population of isomer *rac*-**D** is observed (top to bottom spectra). c) Photoconversion of the isomer mixture *rac*-**C**/*rac*-**D** in MeCN-d_3 solution at 22 °C followed by ^{1}H NMR-spectroscopy (400 MHz). Starting with a mixture of *rac*-**C**/*rac*-**D** (top spectrum) almost exclusive population of isomer *rac*-**A** is observed (top to bottom spectra). d)

Photoconversion of isomers **B** in MeCN solution at -40 °C followed by chiral HPLC. Starting with enantiomerically pure **B** (chromatogram 1) HPLC runs were conducted after different times of continuous irradiation at -40 °C monitoring the photoisomerization process (chromatograms 2-10).

Taking the thermal interconversions and the photoreactions together a repetitive isomerization cycle of racemic HTI **1** can be established in four distinct steps (Figure 5a). Starting with isomer *rac*-**B** the *rac*-**D** isomer can be obtained with 48% in the PSS. By thermal SBR *rac*-**D** is converted into the *rac*-**C** isomer with 86%, as the thermal equilibrium ratio between *rac*-**C** and *rac*-**D** is 86:14. By further irradiation at 20 °C isomer *rac*-**A** can be enriched up to 95% (*rac*-**A**: *rac*-**B**: *rac*-**C**: *rac*-**D** = 95:3:2:0). In the next thermal SBR *rac*-**A** is converted to *rac*-**B** with 78% (*rac*-**A**: *rac*-**B**: *rac*-**C**: *rac*-**D** = 20:78:2:0). Therefore, a complete cycle populating one of the four diastereomers selectively after another is performed by HTI **1**. This cycle can be repeated without isolation of one of the diastereomers by "refocussing" the mixture in the isomer *rac*-**A** enriched state. This is achieved by irradiation of the mixture with 405 nm light at 20 °C, which reestablishes reliably the *rac*-**A**: *rac*-**B**: *rac*-**C**: *rac*-**D** = 95:3:2:0 ratio in solution. Consequently, the following heating and photoisomerization steps produce the same isomer ratios as in the first cycle. The fact that this cycle is reproducible when starting from an arbitrary mixture of isomers of HTI **1** was demonstrated by executing the cycle experiment 3 times in a row with the same NMR-sample (see Supplementary Information). Also, after 10 cycles, corresponding to 20 photochemical and 20 thermal steps, only minimal degradation of the performance by about 5% was observed (Figure 5b).

When also taking the enantiomers into account a selective cycle of isomer interconversions **A→B→D→C→A'→B'→D'→C'→A** is constituted from the main photoreactions and thermal reactions. This is possible because each individual isomer transformation is highly selective under well controlled conditions. The **A→B** and **A'→B'** as well as **D→C** and **D'→C'** interconversions proceed thermally and without racemization as sole SBRs and all photochemical steps proceed as Hula-Twist reactions again with high selectivities. After a total of eight steps the starting isomer is obtained again. This eight-step cycle can however be bypassed by the one-photon-DSBR converting isomer **B** into **B'**. In this case HTI **1** performs the two enantiomeric cycles **A→B→B'→D'→C'→A** and **A'→B'→B→D→C→A'**.

By changing the environmental conditions during photoirradiation steps switching between the five- and eight-step cycles is possible (Figure 5c). If isomers **B** and **B'** perform a Hula-Twist photoreaction the eight-step cycle is followed and if the one photon DSBR occurs one of the five-step cycles is pursued. Obviously, the probability of the eight step-cycle is 100% if both **B** isomers perform exclusively the Hula-Twist reaction. This situation is nearly reached in MeOH solution at -80 °C with a preference for the Hula-Twist reaction of 85% corresponding to 72% eight-step cycle overall (see Figure 5c and the

Supporting Information for calculation details). Optimizing the conditions for the five-step cycle is not so obvious, as both the Hula-Twist and DSBR reaction of **B**/ **B'** are required for this cycle. Maximum efficiency for the five-step cycles is therefore reached in a situation where 50% Hula-Twist and 50% DSBR are present. This situation is reached nearly perfectly in MeCN solution at 20 °C where 61% DSBR and 39% Hula-Twist leads to 48% propensity for the five-step cycle (Figure 5c). At the same time 15% of the eight-step cycle are present under these conditions. Similarly irradiation of **B**/ **B'** at -40 °C in MeCN also leads to 48% propensity for the five-step cycle, owed to 61% Hula-Twist and 39% DSBR photoreactions taking place under these conditions. However, now 35% of the eight-step cycle are also present, which makes this situation less selective. When further increasing the overall DSBR probability by strongly reducing solvent polarity and conducting experiments in toluene solution, the efficiency for the five-step cycles decreases again slightly, as more "unproductive" switching back and forwards between **B** and **B'** is taking place. However, the decrease of the Hula-Twist reaction is much more severe in this case and a comfortable situation can be reached in which the latter is almost completely suppressed. Thus, in toluene solution at 20 °C the eight-step cycle is only present to 8% and the five-step cycle is much more likely with 40%. In this way the preferences of HTI **1** to undergo a specific isomer interconversion cycle can be switched upside down by simply changing solvent and temperatures. The eight-step cycle is preferred 5fold over the five-step cycle in MeOH solvent at -80 °C (i.e. 72% total likelihood for eight-step versus 15% total likelihood for the five-step cycle). The five-step cycle is preferred over the eight-step cycle also by a factor of 5 in toluene solution at 20 °C (8% total likelihood for eight-step versus 40% total likelihood for the five-step cycle).

Although performing sequential switching cycles HTI **1** is not a molecular motor. Obviously both five-step cycles are mirror-symmetric to each other and therefore any partial directional motions cancel each other out. The eight-step cycle possesses no enantiomeric counterpart but a mirror plane that mirrors one half of the cycle with the other one. This situation is comparable with a *meso*-compound, which is achiral despite the presence of stereo information. While one half of the rotations within the eight-step cycle of HTI **1** is forward, the other half must be backwards and both motions cancel each other out (see Figure 5d). However, HTI **1** is also not a simple switch as the forward and backwards motions are not random but follow a specific sequence and are isomer selective. Therefore, we refer to HTI **1** as a sequential switch. Interestingly, under observation with achiral techniques like NMR or UV-Vis spectroscopy the five- and eight-step cycles are indistinguishable and both cycles lead to the same apparent conversion in the sequence *rac*-**A**→*rac*-**B**→*rac*-**C**→*rac*-**D**.

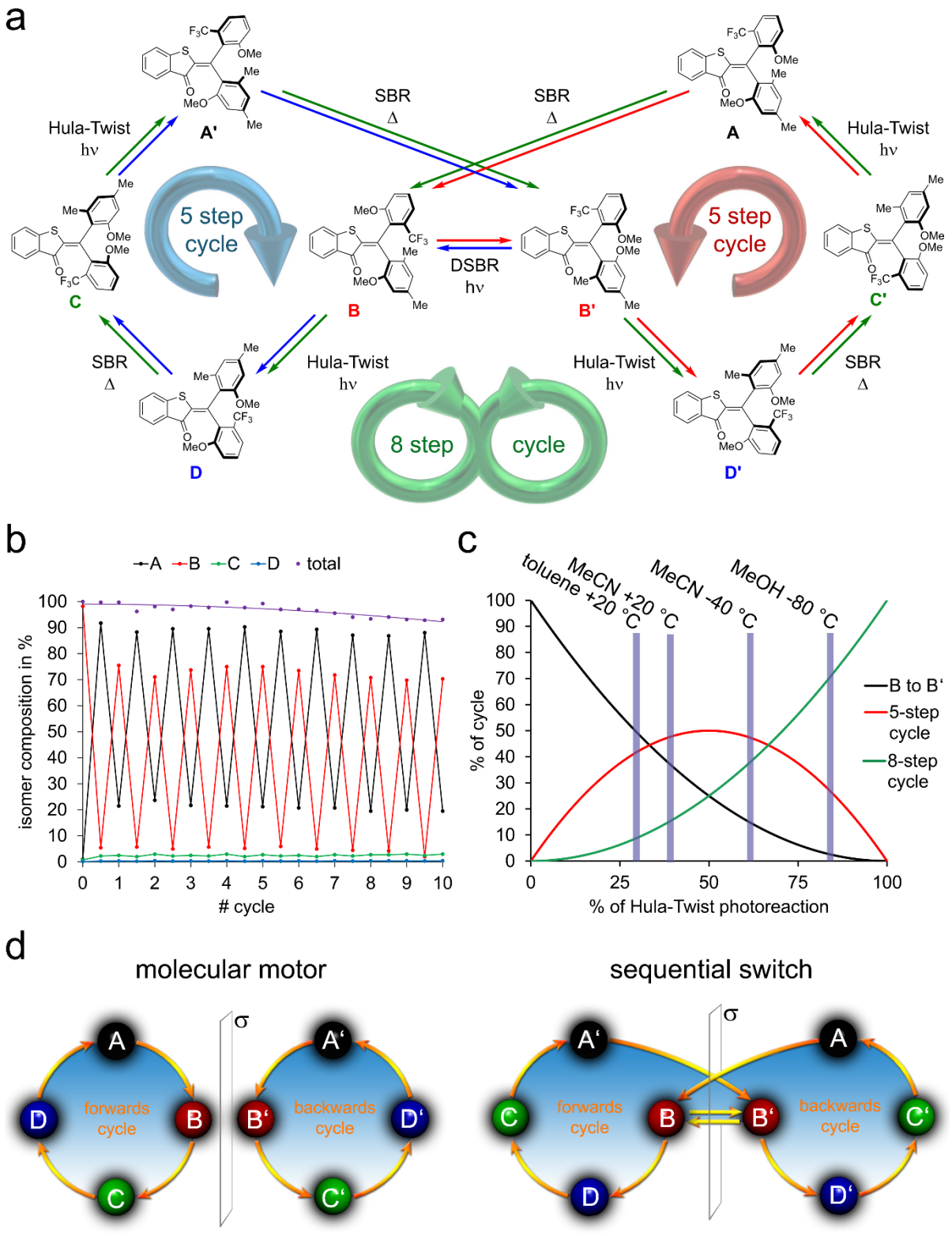

Figure 4 Isomerization properties of the sequential photoswitch **1**. a) Comprehensive scheme showing the selective and sequential switching behavior of HTI **1**. The nature of individual transformations are assigned. b) Repetitive reversible switching cycles of racemic HTI **1**. Minimal loss of performance is observed after 10 full cycles. Refocussing by the same enrichment of isomer *rac*-**A**. c) Propensity for eight- (green trace) or five-step (red trace) sequential switching cycles depending on the ratio of Hula-Twist (x-axis) versus DSBR (black trace) photoreactions of

isomers **B**/**B'**. d) Schematic representation of a molecular motor mechanism as opposed to the herein presented sequential switch mechanism.

In conclusion we herein present an unprecedented type of a sequential molecular switch allowing the interconversion of eight different isomers selectively and in defined sequence. This interconversion can be performed in an eight-step cycle featuring sequential photo activated Hula-Twist reactions and thermal single bond rotations or by two enantiomeric five-step cycles involving an unprecedented one photon DSBR photoreaction. By simply changing solvent and temperature each cycle can be preferred over the other by a factor of five. Furthermore, enrichment of one racemic isomer up to 95% in the PSS is possible enabling a continuous and identical repeatable sequence of isomer interconversions – even when starting with an arbitrary mixture of isomers. This new type of compact molecular tool providing complex sequential movements and eight different accessible states will add new fundamental opportunities for photoswitch applications and future bottom-up building of nanomaterials. In addition, the here discovered one photon DSBR photoreaction enables a new type of light-induced motion at the molecular scale, which should be of great interest for photoswitching applications and especially for future advanced molecular machine building .

Acknowledgements:

H. Dube thanks the Deutsche Forschungsgemeinschaft (DFG) for an Emmy Noether fellowship (DU 1414/1-2). We further thank the European Research Council under the European Union's Horizon 2020 research and innovation program (PHOTOMECH, grant agreement No 101001794, the Deutsche Forschungsgemeinschaft (SFB 749, A12), and the Cluster of Excellence 'Center for Integrated Protein Science Munich' (CIPS^{M}) for further support.

Conflict of interest

The authors declare no conflict of interest.

Keywords: molecular machines • photochemistry • isomerization • hemithioindigo • physical chemistry

References

1. Lubbe, A. S.; Szymanski, W.; Feringa, B. L., Recent developments in reversible photoregulation of oligonucleotide structure and function. *Chem. Soc. Rev.* **2017,** *46* (4), 1052-1079.
2. Lerch, M. M.; Hansen, M. J.; van Dam, G. M.; Szymanski, W.; Feringa, B. L., Emerging Targets in Photopharmacology. *Angew. Chem. Int. Ed.* **2016,** *55* (37), 10978-10999.

3. Velema, W. A.; Szymanski, W.; Feringa, B. L., Photopharmacology: beyond proof of principle. *J. Am. Chem. Soc.* **2014,** *136* (6), 2178-91.
4. Morstein, J.; Trauner, D., New players in phototherapy: photopharmacology and bio-integrated optoelectronics. *Curr. Opin. Chem. Biol.* **2019,** *50*, 145-151.
5. Brieke, C.; Rohrbach, F.; Gottschalk, A.; Mayer, G.; Heckel, A., Light-controlled tools. *Angew. Chem. Int. Ed.* **2012,** *51* (34), 8446-76.
6. Irie, M.; Fukaminato, T.; Matsuda, K.; Kobatake, S., Photochromism of diarylethene molecules and crystals: memories, switches, and actuators. *Chem. Rev.* **2014,** *114* (24), 12174-12277.
7. Andreasson, J.; Pischel, U., Molecules with a sense of logic: a progress report. *Chem. Soc. Rev.* **2015,** *44*, 1053-1069.
8. Shao, B.; Aprahamian, I., Hydrazones as New Molecular Tools. *Chem* **2020,** *6* (9), 2162-2173.
9. Boelke, J.; Hecht, S., Designing Molecular Photoswitches for Soft Materials Applications. *Adv. Optical Mater.* **2019,** *7* (16), 1900404.
10. Göstl, R.; Senf, A.; Hecht, S., Remote-controlling chemical reactions by light: Towards chemistry with high spatio-temporal resolution. *Chem. Soc. Rev.* **2014,** *43* (6), 1982-1996.
11. In *Molecular Switches*, Second ed.; Feringa, B. L.; Browne, W. R., Eds. Wiley-VCH Verlag GmbH & Co. KGaA: 2011.
12. Petermayer, C.; Dube, H., Indigoid Photoswitches: Visible Light Responsive Molecular Tools. *Acc. Chem. Res.* **2018,** *51* (5), 1153-1163.
13. Kortekaas, L.; Browne, W. R., The evolution of spiropyran: fundamentals and progress of an extraordinarily versatile photochrome. *Chem. Soc. Rev.* **2019,** *48* (12), 3406-3424.
14. Hull, K.; Morstein, J.; Trauner, D., In Vivo Photopharmacology. *Chem. Rev.* **2018,** *118* (21), 10710-10747.
15. Klajn, R., Spiropyran-based dynamic materials. *Chem. Soc. Rev.* **2014,** *43* (1), 148-84.
16. Andreasson, J.; Pischel, U., Molecules for security measures: from keypad locks to advanced communication protocols. *Chem. Soc. Rev.* **2018,** *47* (7), 2266-2279.
17. Fischer, E.; Hirshberg, Y., Formation of coloured forms of spirans by low-temperature irradiation. *J. Chem. Soc.* **1952**, 4522-4524.
18. Irie, M.; Mohri, M., Thermally Irreversible Photochromic Systems. Reversible Photocyclization of Diarylethene Derivatives. *J. Org. Chem.* **1987,** *53*, 803-808.
19. Waldeck, D. H., Photoisomerization Dynamics of Stilbenes. *Chem. Rev.* **1991,** *91*, 415-436.
20. Bandara, H. M.; Burdette, S. C., Photoisomerization in different classes of azobenzene. *Chem. Soc. Rev.* **2012,** *41* (5), 1809-25.
21. Weinstein, J.; Wyman, G. M., Spectroscopic Studies on Dyes. II. The Structure of N,N'-Dimethylindigo1. *J. Am. Chem. Soc.* **1956,** *78* (16), 4007-4010.
22. Saltiel, J.; Papadimitriou, D.; Krishna, T. S.; Huang, Z. N.; Krishnamoorthy, G.; Laohhasurayotin, S.; Clark, R. J., Photoisomerization of all-cis-1,6-diphenyl-1,3,5-hexatriene in the solid state and in solution: a simultaneous three-bond twist process. *Angew. Chem. Int. Ed.* **2009,** *48* (43), 8082-5.
23. Gerwien, A.; Schildhauer, M.; Thumser, S.; Mayer, P.; Dube, H., Direct evidence for hula twist and single-bond rotation photoproducts. *Nat. Commun.* **2018,** *9* (1), 2510.
24. Gerwien, A.; Mayer, P.; Dube, H., Photon-Only Molecular Motor with Reverse Temperature-Dependent Efficiency. *J. Am. Chem. Soc.* **2018,** *140*, 16442-16445.
25. Liu, R. S.; Asato, A. E., The primary process of vision and the structure of bathorhodopsin: a mechanism for photoisomerization of polyenes. *Proc. Natl. Acad. Sci. U. S. A.* **1985,** *82* (2), 259-63.
26. Fuß, W.; Kosmidis, C.; Schmid, W. E.; Trushin, S. A., The photochemical cis-trans isomerization of free stilbene molecules follows a hula-twist pathway. *Angew. Chem. Int. Ed.* **2004,** *43* (32), 4178-82.

27. Warshel, A., Bicycle-pedal model for the first step in the vision process. *Nature* **1976,** *260*, 679-683.
28. Schapiro, I.; Weingart, O.; Buss, V., Bicycle-Pedal Isomerization in a Rhodopsin Chromophore Model. *J. Am. Chem. Soc.* **2009,** *131* (1), 16-17.
29. Zhang, Q.; Chen, X.; Cui, G.; Fang, W.-H.; Thiel, W., Concerted Asynchronous Hula-Twist Photoisomerization in the S65T/H148D Mutant of Green Fluorescent Protein. *Angew. Chem., Int. Ed.* **2014,** *53* (33), 8649-8653.
30. Jung, Y. O.; Lee, J. H.; Kim, J.; Schmidt, M.; Moffat, K.; Srajer, V.; Ihee, H., Volume-conserving trans-cis isomerization pathways in photoactive yellow protein visualized by picosecond X-ray crystallography. *Nat. Chem.* **2013,** *5* (3), 212-220.
31. Kaila, V. R. I.; Schotte, F.; Cho, H. S.; Hummer, G.; Anfinrud, P. A., Contradictions in X-ray structures of intermediates in the photocycle of photoactive yellow protein. *Nat. Chem.* **2014,** *6* (4), 258-259.
32. Jung, Y. O.; Lee, J. H.; Kim, J.; Schmidt, M.; Moffat, K.; Šrajer, V.; Ihee, H., Reply to 'contradictions in X-ray structures of intermediates in the photocycle of photoactive yellow protein'. *Nat. Chem.* **2014,** *6*, 259-60.
33. Gust, D.; Andreasson, J.; Pischel, U.; Moore, T. A.; Moore, A. L., Data and signal processing using photochromic molecules. *Chem. Commun.* **2012,** *48* (14), 1947-57.
34. Mutoh, K.; Kobayashi, Y.; Yamane, T.; Ikezawa, T.; Abe, J., Rate-Tunable Stepwise Two-Photon-Gated Photoresponsive Systems Employing a Synergetic Interaction between Transient Biradical Units. *J. Am. Chem. Soc.* **2017,** *139* (12), 4452-4461.
35. Moran, M. J.; Magrini, M.; Walba, D. M.; Aprahamian, I., Driving a Liquid Crystal Phase Transition Using a Photochromic Hydrazone. *J. Am. Chem. Soc.* **2018,** *140* (42), 13623-13627.
36. Fihey, A.; Perrier, A.; Browne, W. R.; Jacquemin, D., Multiphotochromic molecular systems. *Chem. Soc. Rev.* **2015,** *44* (11), 3719-59.
37. Yu, Z.; Weidner, S.; Risse, T.; Hecht, S., The role of statistics and microenvironment for the photoresponse in multi-switch architectures: The case of photoswitchable oligoazobenzene foldamers. *Chem. Sci.* **2013,** *4*, 4156-4167.
38. Zhang, J.; Zou, Q.; Tian, H., Photochromic materials: more than meets the eye. *Adv. Mater.* **2013,** *25* (3), 378-99.
39. Zhao, F.; Grubert, L.; Hecht, S.; Bleger, D., Orthogonal switching in four-state azobenzene mixed-dimers. *Chemical Communications (Cambridge, United Kingdom)* **2017,** *53*, 3323-3326.
40. Bléger, D.; Liebig, T.; Thiermann, R.; Maskos, M.; Rabe, J. P.; Hecht, S., Light-Orchestrated Macromolecular "Accordions": Reversible Photoinduced Shrinking of Rigid-Rod Polymers. *Angew. Chem. Int. Ed.* **2011,** *50* (52), 12559-12563.
41. Heindl, A. H.; Becker, J.; Wegner, H. A., Selective switching of multiple azobenzenes. *Chem. Sci.* **2019,** *10* (31), 7418-7425.
42. Yang, C.; Slavov, C.; Wegner, H. A.; Wachtveitl, J.; Dreuw, A., Computational design of a molecular triple photoswitch for wavelength-selective control. *Chem Sci* **2018,** *9* (46), 8665-8672.
43. Cisnetti, F.; Ballardini, R.; Credi, A.; Gandolfi, M. T.; Masiero, S.; Negri, F.; Pieraccini, S.; Spada, G. P., Photochemical and electronic properties of conjugated bis(azo) compounds: an experimental and computational study. *Chem. Eur. J.* **2004,** *10* (8), 2011-21.
44. Peters, A.; Branda, N. R., Limited photochromism in covalently linked double 1,2-dithienylethenes. *Adv. Mater. Opt. Electron.* **2000,** *10* (6), 245-249.
45. Yagi, K.; Irie, M., Photochromic and Fluorescent Properties of a Diarylethene Dimer. *Chem. Lett.* **2003,** *32* (9), 848-849.
46. Han, M.; Luo, Y.; Damaschke, B.; Gomez, L.; Ribas, X.; Jose, A.; Peretzki, P.; Seibt, M.; Clever, G. H., Light-Controlled Interconversion between a Self-Assembled Triangle and a Rhombicuboctahedral Sphere. *Angew. Chem. Int. Ed.* **2016,** *55* (1), 445-449.

47. Han, M.; Michel, R.; He, B.; Chen, Y. S.; Stalke, D.; John, M.; Clever, G. H., Light-triggered guest uptake and release by a photochromic coordination cage. *Angew. Chem. Int. Ed.* **2013,** *52* (4), 1319-1323.
48. Kortekaas, L.; Ivashenko, O.; van Herpt, J. T.; Browne, W. R., A Remarkable Multitasking Double Spiropyran: Bidirectional Visible-Light Switching of Polymer-Coated Surfaces with Dual Redox and Proton Gating. *J. Am. Chem. Soc.* **2016,** *138* (4), 1301-12.
49. Hoffmann, K.; Guentner, M.; Mayer, P.; Dube, H., Symmetric and nonsymmetric bis-hemithioindigos – precise visible light controlled shape-shifters. *Org. Chem. Front.* **2019,** *6* (8), 1244-1252.
50. Vlasceanu, A.; Koerstz, M.; Skov, A. B.; Mikkelsen, K. V.; Nielsen, M. B., Multistate Photoswitches: Macrocyclic Dihydroazulene/Azobenzene Conjugates. *Angew. Chem. Int. Ed.* **2018,** *57* (21), 6069-6072.
51. Andreasson, J.; Pischel, U.; Straight, S. D.; Moore, T. A.; Moore, A. L.; Gust, D., All-photonic multifunctional molecular logic device. *J. Am. Chem. Soc.* **2011,** *133* (30), 11641-8.
52. Balter, M.; Li, S.; Nilsson, J. R.; Andreasson, J.; Pischel, U., An all-photonic molecule-based parity generator/checker for error detection in data transmission. *J. Am. Chem. Soc.* **2013,** *135* (28), 10230-3.
53. Guerrin, C.; Aidibi, Y.; Sanguinet, L.; Leriche, P.; Aloise, S.; Orio, M.; Delbaere, S., When Light and Acid Play Tic-Tac-Toe with a Nine-State Molecular Switch. *J. Am. Chem. Soc.* **2019,** *141* (48), 19151-19160.
54. Gobbi, L.; Seiler, P.; Diederich, F., A Novel Three-Way Chromophoric Molecular Switch: pH and Light Controllable Switching Cycles. *Angew. Chem. Int. Ed.* **1999,** *38* (5), 674-678.
55. Kink, F.; Collado, M. P.; Wiedbrauk, S.; Mayer, P.; Dube, H., Bistable Photoswitching of Hemithioindigo with Green and Red Light: Entry Point to Advanced Molecular Digital Information Processing. *Chem. Eur. J.* **2017,** *23*, 6237-6243.
56. Koumura, N.; Zijlstra, R. W. J.; van Delden, R. A.; Feringa, B. L., Light-driven monodirectional molecular rotor. *Nature* **1999,** *401*, 152-155.
57. Kassem, S.; van Leeuwen, T.; Lubbe, A. S.; Wilson, M. R.; Feringa, B. L.; Leigh, D. A., Artificial molecular motors. *Chem. Soc. Rev.* **2017,** *46* (9), 2592-2621.
58. Roke, D.; Wezenberg, S. J.; Feringa, B. L., Molecular rotary motors: Unidirectional motion around double bonds. *Proc. Natl. Acad. Sci. U. S. A.* **2018,** *115* (38), 9423-9431.
59. Kistemaker, H. A.; Stacko, P.; Visser, J.; Feringa, B. L., Unidirectional rotary motion in achiral molecular motors. *Nat. Chem.* **2015,** *7*, 890-896.
60. Klok, M.; Boyle, N.; Pryce, M. T.; Meetsma, A.; Browne, W. R.; Feringa, B. L., MHz Unidirectional Rotation of Molecular Rotary Motors. *J. Am. Chem. Soc.* **2008,** *130*, 10484-10485.
61. Štacko, P.; Kistemaker, J. C. M.; van Leeuwen, T.; Chang, M.-C.; Otten, E.; Feringa, B. L., Locked synchronous rotor motion in a molecular motor. *Science* **2017,** *356* (6341), 964-968.
62. Greb, L.; Lehn, J. M., Light-driven molecular motors: imines as four-step or two-step unidirectional rotors. *J. Am. Chem. Soc.* **2014,** *136* (38), 13114-13117.
63. Guentner, M.; Schildhauer, M.; Thumser, S.; Mayer, P.; Stephenson, D.; Mayer, P. J.; Dube, H., Sunlight-powered kHz rotation of a hemithioindigo-based molecular motor. *Nat. Commun.* **2015,** *6*, 8406.
64. Huber, L. A.; Hoffmann, K.; Thumser, S.; Böcher, N.; Mayer, P.; Dube, H., Direct Observation of Hemithioindigo-Motor Unidirectionality. *Angew. Chem. Int. Ed.* **2017,** *56*, 14536-14539.
65. Wilcken, R.; Schildhauer, M.; Rott, F.; Huber, L. A.; Guentner, M.; Thumser, S.; Hoffmann, K.; Oesterling, S.; de Vivie-Riedle, R.; Riedle, E.; Dube, H., Complete Mechanism of Hemithioindigo Motor Rotation. *J. Am. Chem. Soc.* **2018,** *140*, 5311-5318.

66. Gerwien, A.; Mayer, P.; Dube, H., Green light powered molecular state motor enabling eight-shaped unidirectional rotation. *Nat. Commun.* **2019,** *10* (1), 4449.
67. Uhl, E.; Mayer, P.; Dube, H., Active and Unidirectional Acceleration of Biaryl Rotation by a Molecular Motor. *Angew. Chem. Int. Ed.* **2020,** *59* (14), 5730-5737.
68. Gerwien, A.; Reinhardt, T.; Mayer, P.; Dube, H., Synthesis of Double-Bond Substituted Hemithioindigo Photoswitches. *Org. Lett.* **2018,** *1*, 232-235.
69. Liu, R. S. H., Photoisomerization by Hula-Twist: A Fundamental Supramolecular Photochemical Reaction. *Acc. Chem. Res.* **2001,** *34* (7), 555-562.